MATEC Web of Conferences **21**, 02001 (2015)
DOI: 10.1051/matecconf/20152102001

Time-dependent rheoforging of A6061 aluminum alloy on a mechanical servo press and the effects of forming conditions on homogeneity of rheoforged samples

Yi Meng[1,2,a], Sumio Sugiyama[2], and Jun Yanagimoto[2]

[1] Department of Materials Engineering, School of Engineering, The University of Tokyo, Hongo 7-3-1, Bunkyo-ku, Tokyo, Japan
[2] Institute of Industrial Science, The University of Tokyo, Meguro 4-6-1, Komaba-ku, Tokyo, Japan

Abstract. The solid and liquid phases in semisolid metal slurry exhibited different forming behaviours during deformation result in products with inhomogeneous quality. A6061 aluminum alloy was forged in the semisolid state on a mechanical servo press with the capability of multistage compression. To improve the homogeneity of rheoforged samples a time-dependent rheoforging strategy was designed. The distributions of the microstructure and mechanical properties the samples manufactured under various experimental conditions were investigated. The A6061 samples forged in the temperature range from 625 to 628 °C with a short holding time of 4 s and the upper die preheated to 300 °C exhibited a homogeneous microstructure and mechanical properties. The homogeneity of rheoforged samples resulted from the controllable free motion capability of the mechanical servo press and the adjustable fluidity and viscosity of the semisolid slurry.

1. Introduction

Since semisolid forming (SSF) technology was invented in 1970s, it attracts more attention than conventional forming methods, owing to the unique characteristics of a semisolid-state metal including excellent fluidity, adjustable viscosity, and controllable morphology [1]. Mechanical servo presses combining the flexibility of a hydraulic press and the reliability of a mechanical press, are widely applied in metal forming [2]. Compared with the conventional hydraulic machines, the mechanical servo presses exhibit several advantages including higher product accuracy, better machine reliability, and less noise [3]. Owing to the controllable free motion capability of a mechanical servo press, it can be employed to manufacture two types of aluminum alloy samples with homogeneous microstructure in semisolid state [4]. However, further research should be carried out to reveal the relationship between semisolid forming conditions and the microstructure and mechanical properties of samples manufactured by semisolid forming technology.

[a] Corresponding author: meng@sip-mi.t.u-tokyo.ac.jp

Table 1. Chemical composition of A6061-T6 aluminum alloy used in experiments (mass%).

Si	Fe	Cu	Mn	Mg	Zn	Ti	Cr	Al
0.4–0.8	≦ 0.7	0.15–0.4	≦ 0.15	0.8–1.2	≦0.25	≦ 0.15	0.04–0.35	Bal.

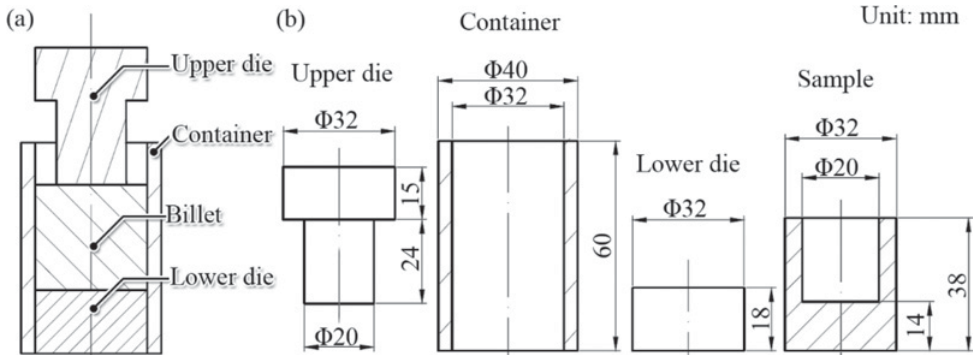

Figure 1. An illustration of people working in a factory.

In this study, with the aim of, an effective time-dependent rheoforging strategy on a mechanical servo press is established to manufacture non-ferrous samples with a homogeneous properties. The microstructural evolution of A6061 aluminum alloy during time-dependent rheoforging and the effects of forming conditions on the homogeneity of microstructure were investigated by rapid-cooling and observation experiments. The effects of forming conditions on the homogeneity of mechanical properties of the samples manufactured by time-dependent rheoforging were investigated by Vickers hardness measurements and compression tests.

2. Experimental procedure

The chemical composition of the A6061-T6 aluminum alloy used in this study is shown in Table 1. To obtain globular semisolid slurry the molten A6061-T6 alloy was mechanically stirred at a speed of 80 rev/s during cooling. The semisolid slurry was rheoforged at 625, 628, 631, and 634 °C on a mechanical servo press with a maximum forming load of 40 KN. On the basis of the differential scanning calorimetry (DSC) analysis result, the solid fractions of these specimens were between 43, 30, 21, and 12%, respectively. The schematic diagram of experimental setup, dimensions of dies and sample made from SKD61 tool steel are shown in Fig. 1. The upper dies at room temperature, 200, and 300 °C were used. The motion of the mechanical servo press during the time-dependent rheoforging including fast first compression, short holding, and slow secondary compression is shown in Fig. 2.

To evaluate the microstructure and mechanical properties of various regions of the rheoforged sample, each sample was divided into four parts as shown in Fig. 3. The microstructure of rapid-cooled samples were observed by optical microscopy after polishing and etching. The Vickers hardness tests were conducted with a load of 0.2 kg and a dwell time of 10 s. Compress tests of cylindrical specimens (ϕ6 mm × 9 mm) cut from the four parts of rheoforged samples were carried out with a height reduction of 50% at room temperature in accordance with ASTM E9-09.

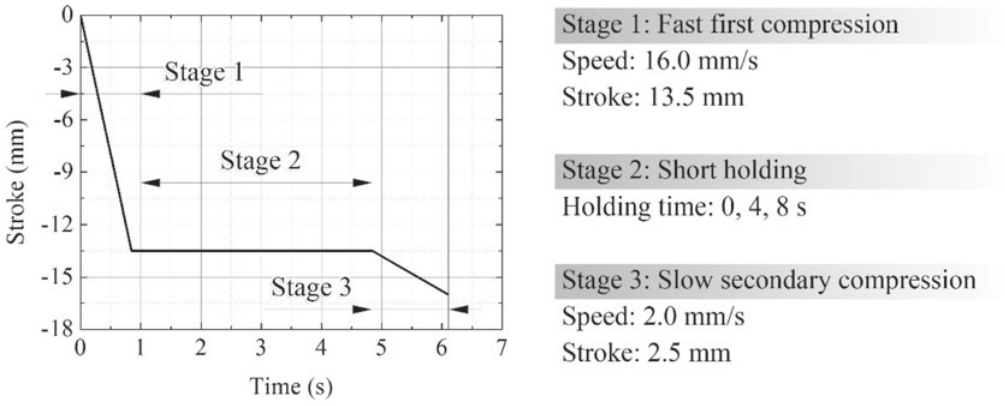

Figure 2. The motion of the mechanical servo press during the time-dependent rheoforging.

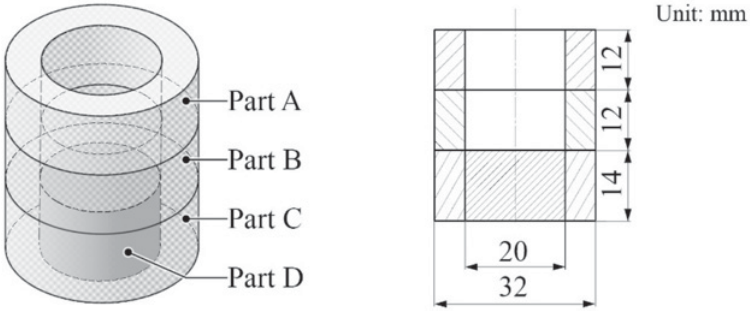

Figure 3. An illustration of the partitioning of the rheoforged sample.

3. Results and discussion

3.1 Time-dependent rheoforging

Figure 4 shows the measured forming load-stroke and temperature-stroke curves of time-dependent rheoforging carried out at 625 °C with a short holding time and a upper die temperature of 4 s and 400 °C, respectively. The three stages of time-dependent rheoforging could be distinguished from each other by their difference profiles.

To investigate the mechanism of time-dependent rheoforging, the samples were cooled rapidly at the end of every stage to observe the frozen microstructure. According to the solid fraction estimated by image analysis software shown in Fig. 5, the phase segregation occurred in fast first compression was slight. In this stage, the higher shear rate decreased the agglomeration of globular solid particles and ensured the excellent formability of the semisolid slurry. The higher fluidity of the semisolid alloy slurry with a lower solid fraction resulted in the lower forming load in this stage. Owing to conduction between the sample and the dies, the temperature of semisolid slurry thermal decreased. The decrease in temperature caused an increase in the solid fraction and a gradual increase in the forming load as shown in Fig. 4. The different forming behaviours of the liquid phase and solid phase caused the phase segregation. In the short holding stage, no compression was conducted. The forming load dropped to 0 and the temperature of semisolid slurry decreased by about 15 °C. During the short holding for 4 s, increase of solid fraction was attributed to the combination of solid particles with the ones surround them. This microstructural evolution was mainly attributed to the partial solidification of the liquid

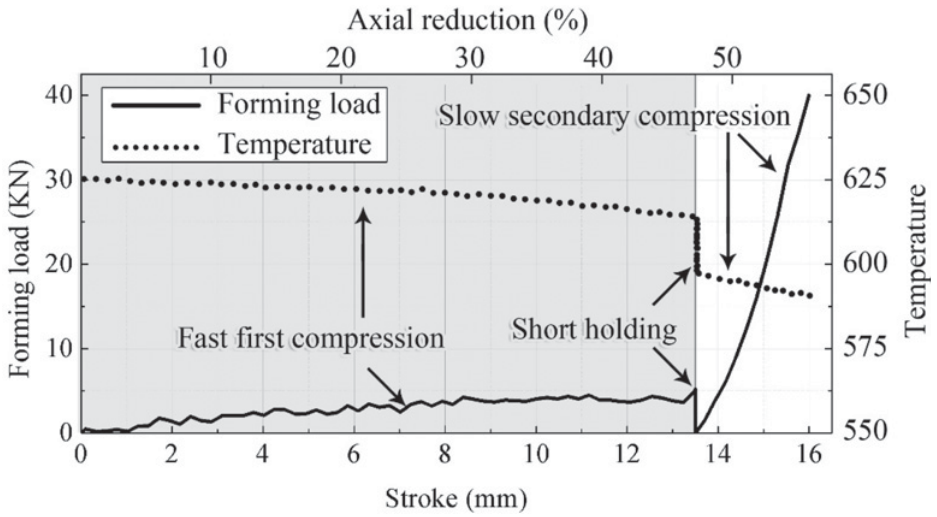

Figure 4. Forming load-stroke and temperature-stroke curves of time-dependent rheoforging.

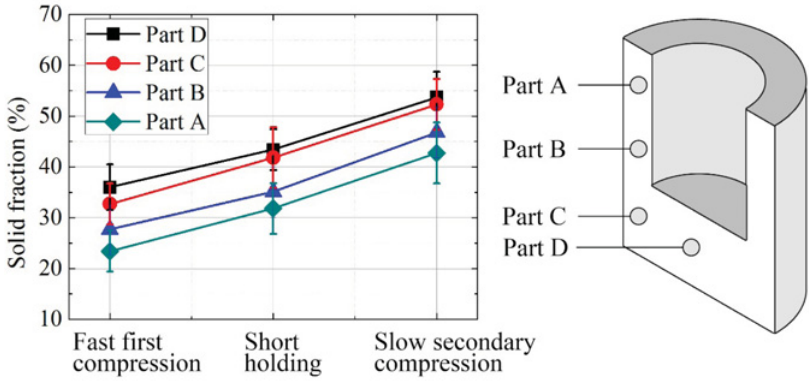

Figure 5. Solid fractions of various regions of samples cooled rapidly at the end of various stages.

phase in this stage. In the Slow secondary compression, the partial dendritic solidification of liquid phase and combination of solid particles continued owing to the lower strain rate. The semisolid alloy slurry with a higher solid fraction and a rosette morphology exhibited lower fluidity and higher deformation resistance [5]. Owing to the less fluidity and higher solid fraction of the semisolid slurry, further phase segregation was inhibited in the slow secondary compression.

3.2 Effects of forming conditions

The macroscopic profiles and micrographs of samples manufactured at 625 °C by time-dependent rheoforging with various short holding times are shown in Fig. 6. The aim of short holding is to prevent further phase segregation by increasing the solid fraction of the semisolid slurry. When the holding time was too short, the semisolid slurry still exhibited high fluidity. The lower forming speed in the secondary compression provides a longer time for the outflow of the liquid phase causing greater phase segregation. Defect was observed on the sample formed by the time-dependent rheoforging without

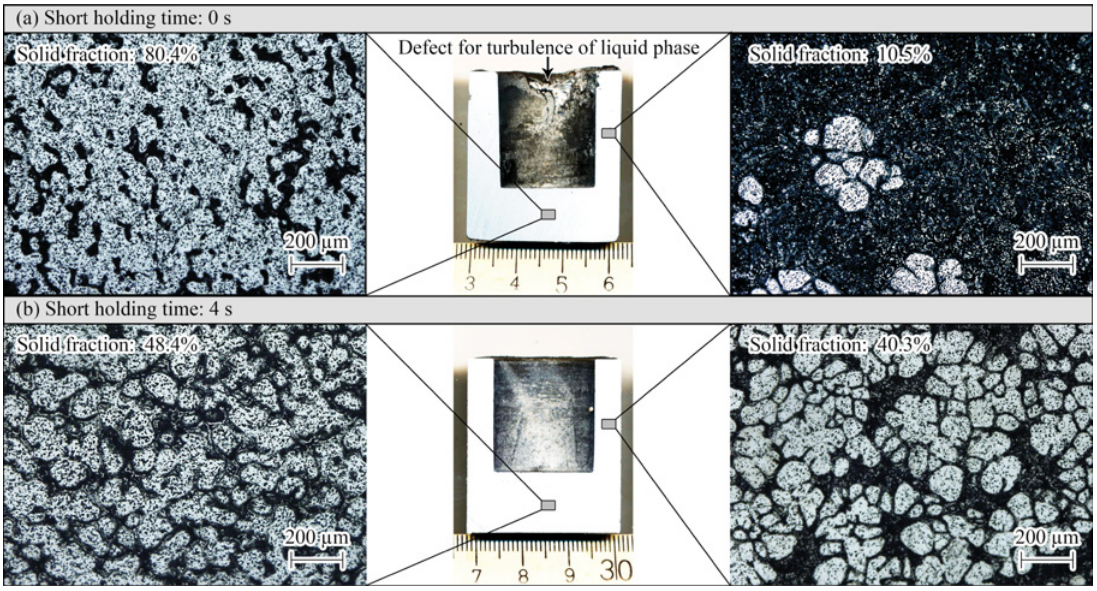

Figure 6. Macrographs and micrographs of samples forged at 625 °C with various holding times.

short holding. When the short holding time was 4 s, sample without macro-defect was obtained. At a higher rheoforging temperature, the higher fluidity of the semisolid slurry causes more serious phase segregation [6]. The phase segregation occurred in the fast first compression cannot be adjusted in the subsequent stages. In the secondary compression, a high forming speed causes turbulence of the liquid phase, resulting in casting defects, but a low forming speed exacerbates the phase segregation. After rapid cooling, shrinkage occurred in the regions of samples with a lower solid fraction, as shown in Fig. 7.

The yield stress and Vickers hardness of various regions of samples rheoforged under different experimental conditions. To evaluate the homogeneity of the Vickers hardness of the specimens, the standard deviation was employed:

$$S = \sqrt{\frac{\sum (x_i - \bar{x})^2}{n - 1}} \tag{1}$$

where S is the standard deviation, x_i is the measured value, $\bar{x}$ is the average value, and n is the number of measured values. The standard deviation of the measured mechanical properties of samples rheoforged under different experimental conditions is shown in Table 2.

The homogeneity of mechanical properties of samples forged under different conditions was attributed to their different morphologies. The mechanical properties of the parts with a finer globular microstructure are superior to those of the parts with a coarser rosette microstructure [7]. The regions with a lower solid fraction exhibited lower yield strength and higher hardness. The higher hardness of liquid-phase regions resulted from the smaller particles of aluminum with a dendritic-structure, eutectic and intermetallic located in these regions [8]. The lower deformation resistance of the parts with a lower solid fraction was attributed to the defects in the liquid-phase regions, such as porosities and shrinkage. These defects resulted from the aggregation of the liquid phase during rheoforging and the subsequent cooling. On the basis of the obtained experimental results, The samples rheoforged in the temperature

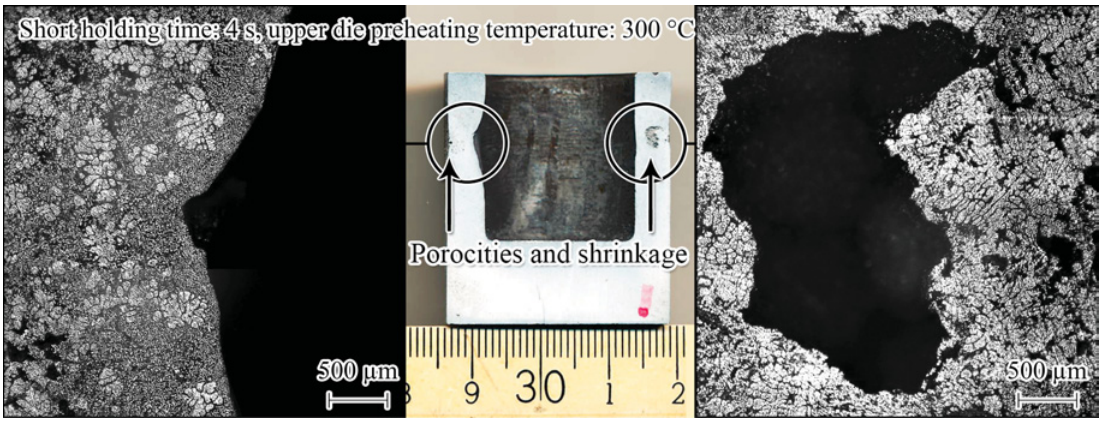

Figure 7. Macrograph and micrographs of the sample rheoforged at 634 °C.

Table 2. Standard deviation of mechanical properties of samples forged under different conditions.

Forging temperature (°C)	Short holding time (s)	Upper die temperature (°C)	Standard deviation of yield strength (MPa)	Standard deviation of Vickers hardness (HV)
625	0	300	20.77	71.64
625	4	300	4.27	6.27
625	8	300	7.94	7.24
625	4	20	92.98	92.86
625	4	200	17.10	31.62
628	4	300	5.48	8.54
631	4	300	21.00	67.21
634	4	300	27.53	84.59

range of 625 ∼ 628 °C with a short holding time of 4 s and a upper die temperature of 400 °C exhibit the most homogeneous mechanical properties.

4. Conclusion

The main results of this study are summarized as follows.

- The feasibility of a time-dependent rheoforging strategy conducted on a mechanical servo press was verified experimentally. A6061-T6 aluminum alloy sample with simple geometric shape was manufactured successfully by this forming strategy.
- During time-dependent rheoforging different microstructural evolutions occurred in different stages including fast first compression, short holding, and slow secondary compression.
- Sample with homogeneous microstructure and mechanical properties could be manufactured when forming temperature range, short holding time, and upper die temperature were 625 to 628 °C, 4 s, and 400 °C, respectively.

This study was financially supported by a Grant-in-Aid for Scientific Research on Innovative Area, “Bulk Nanostructured Metals” through MEXT, Japan (contract No. 22102005) and an Encouraged Research through Amada Foundation, Japan (contract No. AF-2014032).

References

[1] H. Atkinson, A. Rassili, *Thixoforming steel* (Shaker Verlag, Aachen, 2010)
[2] R. Matsumoto, J. Jeon, H. Utsunomiya, J. Mater. Process. Technol. **213**, 770 (2013)
[3] K. Osakada, K. Mori, T. Altan, P. Groche, CIRP Ann. Manuf. Technol. **60**, 651 (2011)
[4] J. Yanagimoto, J. Tan, S. Sugiyama, Y. Meng, Mater. Trans. **54**, 1149 (2013)
[5] Y. Meng, S. Sugiyama, J. Tan, J. Yanagimoto, J. Mater. Process. Technol. **214**, 3039 (2014)
[6] P.K. Seo, S.W. Youn, C.G. Kang, J. Mater. Process. Technol. **130–131**, 555 (2002)
[7] Q. Chen, B. Yuan, J. Lin, X. Xia, Z. Zhao, D. Su, J. Alloys Compd. **584**, 73 (2014)
[8] E. Giraud, M. Suéry, M. Coret. Mater. Sci. Eng. A **532**, 41 (2012)